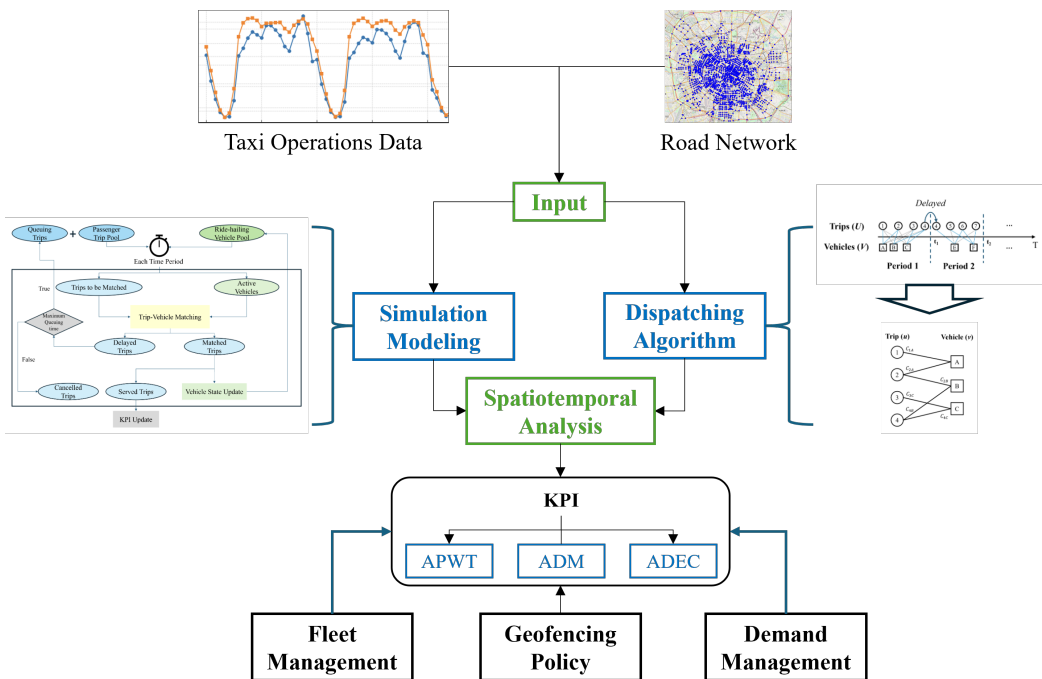


Graphical Abstract

Assessing On-Demand Mobility Services and Policy Impacts: A Case Study from Chengdu, China

Youkai Wu, Zhaoxia Guo, Qi Liu, Stein W.Wallace



Highlights

Assessing On-Demand Mobility Services and Policy Impacts: A Case Study from Chengdu, China

Youkai Wu, Zhaoxia Guo, Qi Liu, Stein W. Wallace

- Compare two on-demand mobility modes based real and identical taxi operations data.
- Evaluate ride-hailing performance using simulation and graph-based algorithms.
- Simulate on-demand automated services with centralized control and direct parking.
- Consider passenger experience, traffic, and energy use as key performance metrics.
- Assess supply- and demand-side policy impacts on ride-hailing performance.

Assessing On-Demand Mobility Services and Policy Impacts: A Case Study from Chengdu, China

Youkai Wu^{a,b}, Zhaoxia Guo^a, Qi Liu^{a,*}, Stein W.Wallace^{a,b}

^a*Business School, Sichuan University, Chengdu, 610065, China*

^b*NHH Norwegian School of Economics, Bergen, Norway*

Abstract

The rapid expansion of ride-hailing services has significantly reshaped urban on-demand mobility patterns, but it still remains unclear how they perform relative to traditional street-hailing services and how effective are related policy interventions. This study presents a simulation framework integrating a graph theory-based trip-vehicle matching mechanism with real cruising taxi operations data to simulate ride-hailing services in Chengdu, China. The performances of the two on-demand mobility service modes (i.e., ride-hailing and street-hailing) are evaluated in terms of three key performance indicators: average passenger waiting time (APWT), average deadheading miles (ADM), and average deadheading energy consumption (ADEC). We further examine the impacts of spatiotemporal characteristics and three types of policies: fleet size management, geofencing, and demand management, on the performance of ride-hailing services. Results show that under the same fleet size and trip demand as street-hailing taxis, ride-hailing services with-

*Corresponding author

Email addresses: youkai.wu@nhh.no (Youkai Wu), zx.guo@alumni.polyu.edu.hk (Zhaoxia Guo), liuqi_67@scu.edu.cn (Qi Liu), stein.wallace@nhh.no (Stein W.Wallace)

out cruising achieve substantial improvements, reducing APWT, ADM, and ADEC by 81%, 75%, and 72.1%, respectively. These improvements are most pronounced during midnight low-demand hours and in remote areas such as airports. Our analysis also reveals that for ride-hailing service, (1) expanding fleet size yields diminishing marginal benefits; (2) geofencing worsens overall performance while it improves the performance of serving all trips within the city center; and (3) demand-side management targeting trips to high-attraction and low-demand areas can effectively reduce passenger waiting time without increasing deadheading costs.

Keywords: On-demand Mobility, Ride-hailing, Spatiotemporal Analysis, Simulation Modeling, Policy Analysis

1. Introduction

Ride-hailing and street-hailing are two typical on-demand mobility service modes in urban areas. Ride-hailing is a digitally enabled service based on automated dispatching systems, in which algorithmic systems pair the request with a nearby driver operating a private vehicle. A ride-hailing service provided by autonomous vehicles is commonly known as an Autonomous Mobility-on-Demand (AMoD) service [1, 2]. In contrast, street-hailing denotes the traditional process of requesting a taxi by visually identifying and signaling a cruising taxi on the street without digital coordination or reservation. Drivers typically cruise or park within designated zones and accept hails directly from pedestrians [3]. Besides, there are other types of traditional taxi service including taxicab stands, or phone central dispatch offices [4]. Over the past decade, ride-hailing services have gradually taken the place

of street-hailing, rapidly reshaping urban on-demand mobility in many cities. The size of the cruising taxi fleet in Shanghai, China, has decreased from over 49,000 in 2015 to around 30,900 in 2024, mainly due to the emergence of ride-hailing services [5, 6]. However, empirical studies have pointed out certain drawbacks of ride-hailing services, particularly too many deadheading miles traveled, which is called the “wild goose chasing” phenomenon [7, 8].

Assessing the performance of ride-hailing services — and their comparison with street-hailing services — is critical for evaluating the value of automated dispatching systems, developing targeted policies to improve the performance of on-demand mobility and passenger experience, and further assessing the economic viability and policy implications of Autonomous Mobility-on-Demand (AMoD) systems [9, 10]. Most existing studies on the comparison of ride-hailing and street-hailing services were conducted based on empirical analysis [3, 11, 12]. Some studies employ simulation-based approaches to solve the problem, but these works have not considered some critical features, such as real urban road networks and dynamic vehicle availability. Meanwhile, several major cities around the world have introduced policies targeting ride-hailing services [13], but their effectiveness remains inconclusive. In particular, limited attention has been paid to evaluate the impacts of both supply- and demand-side policies on ride-hailing services. Given these gaps, this study focuses on two major questions to policymakers:

1. Which service, ride-hailing or street-hailing, performs better? Do ride-hailing services have different performances under different spatiotemporal conditions?
2. How do policy interventions that adjust supply-demand levels and op-

erating areas effect the performance of ride-hailing services?

To answer these questions, this study is conducted by taking Chengdu, a megacity in China, as a case city. First, we develop a simulation framework grounded in real cruising taxi operations data to evaluate and compare ride-hailing and street-hailing services. Second, we formulate the minimization of the passenger pick-up time as the objective function and employ theoretically optimal and efficient graph theory-based trip-vehicle matching mechanisms to simulate ride-hailing services within rolling time windows. We further test three policy interventions, fleet size management, geofencing and demand management, within this framework to analyse their impacts on ride-hailing performances.

This study contributes to the literature in the following ways: i) it is the first to assess the performance of different on-demand mobility services (i.e., ride-hailing and street-hailing services) under the same supply and demand conditions, based on a real taxi operations dataset on an urban road network, ii) it identifies how ride-hailing performance varies across different spatial and temporal conditions, and iii) it simulates and evaluates the impacts of three representative policy interventions (i.e., fleet size management, geofencing, and demand management) on the performance of ride-hailing services.

The remainder of the paper is organized as follows. Section 2 reviews the relevant literature. Section 3 describes the methodology and data used in this study. Section 4 compares results of street-hailing and ride-hailing services based on spatiotemporal analyses. Section 5 discusses the effects of different policy interventions. Section 6 summarizes the main conclusions and outlines future research directions.

2. Literature review

The emergence of ride-hailing services has prompted extensive debate and attracted increasing attention from researchers and policymakers [11, 14, 15]. This section reviews previous studies on (i) the comparison of ride-hailing and street-hailing services, and (ii) the effects of policy interventions on ride-hailing services.

2.1. Comparison of ride-hailing and street-hailing services

Numerous studies have evaluated and compared the performance of ride-hailing and street-hailing services based on different analytical methods, which can be mainly divided into survey-based analyses, empirical data analyses, and model simulation analyses. Some researchers adopted survey-based analyses with structural equation modeling-based methods to examine user adoption and loyalty across street-hailing and ride-hailing services [16, 17]. However, research based on surveys suffers from sampling and response bias. Due to the subjective nature of passenger perceptions, these studies only provided qualitative insights.

To obtain quantitative results, a number of researchers have turned to empirical data analyses to compare ride-hailing and street-hailing services based on real-world operations data (e.g., trip records, GPS trajectories, or household travel surveys). In these studies, regression models have been widely used, including ordinary least squares fixed-effects panel regression, as well as spatial and spatiotemporal econometric methods like spatial autoregressive models and geographically and temporally weighted regression (GTWR). Zhai et al. [18] developed a multivariate conditional autoregressive model

with measurement errors using Chicago census-tract 2019 exposure data. They found that ride-hailing exhibited a higher risk of minor-injury crashes than street-hailing, with no significant difference in severe-injury risk, utilizing data from both ride-hailing and street-hailing services. Luo et al. [19] and Wang et al. [9] applied GTWR models in Beijing and Chicago, respectively, to examine the spatiotemporal dynamics of street-hailing and ride-hailing services using both street-hailing and ride-hailing operations data from these two cities. They found that street-hailing services outperformed ride-hailing in specific areas and periods.

Clustering analysis (e.g., K-means) is also a common method in empirical data analyses to identify diverse groups of ride-hailing users with systematic differences in trip frequency, spatiotemporal pattern, ride-splitting propensity, and modal substitution. Using data from street-hailing and ride-hailing services in Xiamen [20], Chicago [21], and California [22], researchers investigated the differences in passenger travel behavior and policy regulations between street-hailing and ride-hailing services. Although these empirical data analyses constitute the majority of comparative research on ride-hailing and street-hailing services, the major limitation is that they used separate datasets for comparison and failed to provide a fair observation.

To mitigate the bias introduced by different datasets, some researchers adopted model simulation analyses using the same dataset to evaluate the performance of different on-demand mobility services. Vazifeh et al. [23] modeled the operation of autonomous vehicles based on graph theory using data from street-hailing taxis in New York and addressed the minimum fleet problem in on-demand mobility. They also compared the performance of

their autonomous fleet with that of street-hailing taxis and found that their autonomous fleet could serve most trips with fewer vehicles. Feng et al. [24] constructed a queuing network on a closed circular road and simulated the efficiency of point-to-point on-demand matching system under varying demand levels and travel distances. They found that under medium demand and long travel distances, their point-to-point on-demand system performed worse than traditional street-hailing services. These studies compared different on-demand mobility services using the same datasets. However, they either adopted simplified or synthetic spatial environments that did not fully reflect real-world road network constraints or ignore the operational realities (e.g., vehicle availability) in ride-hailing services. They also did not explore the impacts of different spatiotemporal features of ride supply and demand on the performance of ride-hailing services. Thus, the applicability of their findings to ride-hailing services in real urban conditions is limited, especially in megacities with highly complex transportation networks and service demands.

2.2. Policy impacts on ride-hailing services

Previous studies have investigated the impact of a series of policy interventions on ride-hailing services from both the supply and demand sides. Supply-side policies primarily targeted the operational behavior of platforms and drivers, mainly including fleet size management and geofencing (i.e., limiting service areas). Studies showed that a reduced fleet size can serve a similar number of trips under centralized dispatch compared to street-hailing [23, 25, 26]. Beojone et al. [27] utilized street-hailing data from a Chinese megacity and simulated with a trip-based macro-level fundamental

diagram model, demonstrating that while expanding ride-hailing fleets reduced passenger wait times, it increased total travel time by around 37% due to cruising and congestion. They also found that coordination mechanisms, such as the deadheading vehicle management, could reduce the increased total travel time by 7%. However, these studies about fleet size management assumed a constant fleet size throughout the entire day, without considering temporal variations in vehicle availability. Platform-level interventions, such as limiting autonomous vehicle service areas, have also been modeled to explore equilibrium solutions in mixed or monopolistic markets [28]. Liang et al. [29] used a Difference-in-differences (DiD) approach to test the causal effects of vehicle geofencing policies on traffic congestion in Shanghai. However, studies on geofencing policies focused primarily on their impacts on overall traffic congestion, rather than on the performance of ride-hailing services.

Demand-side policies mainly aim to guide, regulate, stimulate, or restrict passenger travel demands. Empirical evaluations [30] using causal inference methods, including DiD and regression discontinuity, indicated that higher congestion fees could reduce demand for ride-hailing and shifted some travelers to alternatives such as public transit or cycling, though its effectiveness varied across cities and could disproportionately burden low-income users. Some simulation results [31] indicated that demand-oriented mechanisms, such as dynamic fare adjustments and price-based prioritization, could help optimize system efficiency and welfare under different traffic conditions. Moreover, research [32] demonstrated that peak-hour pricing could improve dispatch efficiency and platform revenue, but it might also exacerbate driver income inequality and passenger dissatisfaction. Overall, research

on demand management policies has mainly focused on the effectiveness of individual policies, such as dynamic pricing or congestion charges, while limited attention has been paid to the direct effects of demand management on ride-hailing performance and to the trip types that demand management policies should address.

In summary, the major research gaps are as follows. First, the literature lacks a fair comparison of ride-hailing and street-hailing performance using the same real-world dataset while considering the dynamics and complexity of the real-world road networks. Second, most existing studies assess geofencing impacts on ride-hailing through post-policy data, while demand management research mainly focuses on methodological approaches for peak shaving. Previous studies have not evaluated geofencing policies *ex ante* nor identified which types of demand should be adjusted. To fill these research gaps, referring to the research by Vazifeh et al. [23], we employ a simulation-based model to evaluate the performance of ride-hailing services and compare it with the street-hailing performance using the same taxi operations dataset on a real megacity road network. We also evaluate the individual impacts of time-varying fleet size adjustments, geofencing, and demand management policies on the operational performance of ride-hailing services.

3. Methodology and data

In this section, we propose a ride-hailing simulation framework in which trips and ride-hailing vehicles are matched in every time period (e.g., each minute), using a graph theory-based mechanism. Based on the simulation framework, we conduct a case study to compare the performance of

ride-hailing and street-hailing services on three key performance indicators (KPI) using a real cruising taxi operations dataset from the road networks of Chengdu, China.

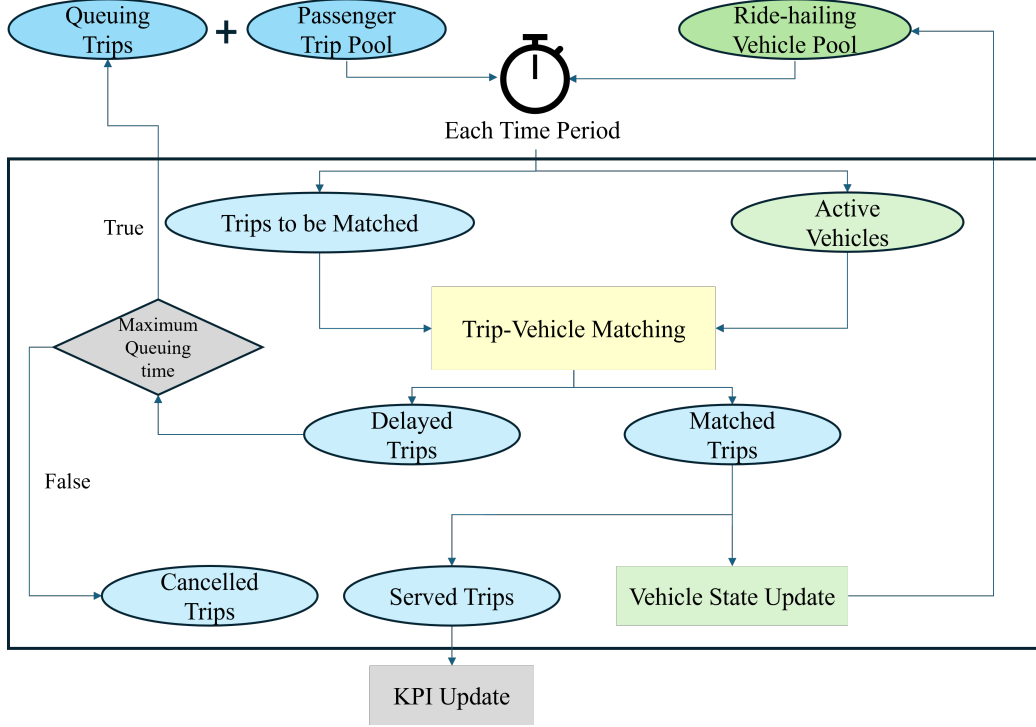


Figure 1: Process of the ride-hailing simulation framework.

3.1. The Ride-hailing simulation framework

Figure 1 shows the simulation framework used to evaluate the performance of ride-hailing services based on an urban road network. We consider two types of entities: trips and ride-hailing vehicles. The trip pool comprises all trips occurring over a single day, according to the historical dataset or generated from a probability distribution. The ride-hailing vehicle pool contains all vehicles operating on a day. For each time period, the set of trips

to be matched is composed of the newly occurred trips together with the unmatched trips from the previous period, and these trips are matched against the active vehicles according to the trip-vehicle matching mechanism. If a trip is successfully matched in the current period, it is then classified as a matched trip, waiting for a vehicle to pick it up, and finally regarded as a successfully served trip. If a trip is not matched, it is set as a delayed trip. A delayed trip is cancelled by the passenger if it has queued for longer than the maximum passenger queuing time, otherwise, it is regarded as a backlogged trip and matched in the next period. The vehicle state is updated according to the actual situation (e.g., picking-up, carrying) at the end of the period. At last, the KPI values are then calculated and renewed.

Table 1: Attributes of ride-hailing vehicles and passengers

| Entity | Attribute | Symbol | Description |
|---------|-----------------|--------------------|---|
| Vehicle | Identification | v | Unique ID of the vehicle. |
| | State | s_t^v | State of vehicle v at period t : {0: Resting, 1: Vacant, 2: Picking-up, 3: Carrying}. |
| | Location (node) | n_t^v | Location (current node) of vehicle v on the road network before period t . |
| Trip | Identification | u | Unique ID of the trip. |
| | State | s_t^u | State of trip u at period t : {0: In queue, 1: Waiting, 2: In transit}. |
| | Request time | t_{req}^u | Time of trip u getting into the matching system. |
| | Origin | o_u | Origin node of the trip u . |
| | Destination | d_u | Destination node of the trip u . |
| | Queuing delay | δ_u^{queue} | Time spent in the queue of trip u . |
| | Pickup delay | δ_u^{pu} | The actual time of trip u taken from being matched to picked up. |

Entity attributes of ride-hailing vehicles and passengers are shown in Table 1 and the parameters of the ride-hailing system that defines platform constraints are summarized in Table 2. These parameters are either fixed or used as control inputs in simulation experiments. We assume that pas-

Table 2: Parameters of the ride-hailing system

| Parameter Name | Symbol | Description |
|-------------------|--|---|
| Fleet size | F | Total number of ride-hailing vehicles in the system. |
| Vehicles by state | $N_{\text{rest}}, N_{\text{vac}}, N_{\text{pu}}, N_{\text{car}}$ | Number of vehicles in resting, vacant, picking-up, and passenger-carrying states. |
| Trip set | O | Set of all trips occurring on a single day. |
| Matching interval | $period$ | Time interval between successive batch matching operations. |
| Max pickup time | t_{pu}^{\max} | Maximum time limit for a vehicle to pick up a trip. |
| Max queue time | t_{queue}^{\max} | Maximum time for a passenger willing to wait in the queue for matching. |

sengers cancel their trips if the queuing delay δ_u^{queue} exceeds the maximum threshold t_{queue}^{\max} . A trip-vehicle pair (u, v) is considered feasible if it satisfies the following criteria : (1) Queuing delay $\delta_u^{\text{queue}} \leq t_{\text{queue}}^{\max}$ and (2) Pickup delay $\delta_u^{\text{pu}} \leq t_{\text{pickup}}^{\max}$.

The urban transportation network is represented as a directed graph $G = (N, E)$, where N denotes the set of road intersection nodes. The origin and destination of each trip are matched to the nearest road intersection node. Meanwhile, $E \subseteq N \times N$ represents the set of directed road edges connecting nodes in N . Each edge is associated with a travel cost (e.g., travel time, length or energy consumption), typically derived from real road and travel data, or directly from historical speed or time data. During the simulation, vehicles in the resting or vacant states park at the destination nodes of their last trip.

3.2. Trip-Vehicle matching

We use a batch strategy (called a batch matching) which aggregates trips within each fixed period (e.g., every 1 minute) to match trips and vehicles in each period sequentially. Through this, we transformed the trip-vehicle

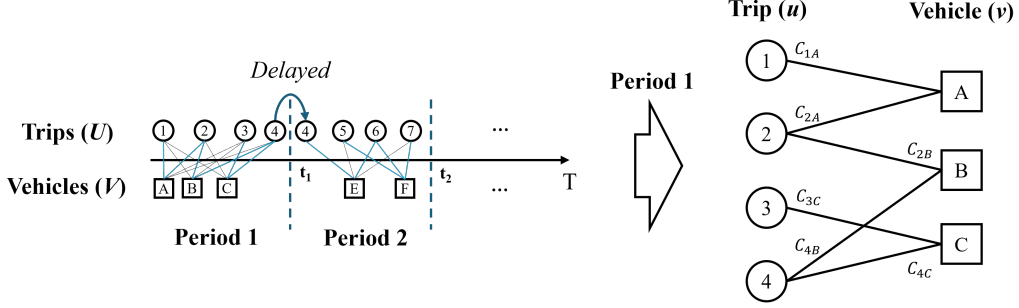


Figure 2: Illustration of the batch matching process. Trips and vehicles are collected within a period. The feasible pairs make up a bipartite graph representing an assignment problem.

matching problem into a bipartite matching and solve it with an algorithm based on graph theory. The objective of batch matching is to minimize the total pickup delay, which is consistent with the setting in the literature [33]. Let U denote the set of trips to be matched in the current period and V denote the set of available ride-hailing vehicles. Figure 2 illustrates the batch matching process. In each period, trips accumulated within the current batch are filtered by t_{pu}^{\max} for the match feasibility, and then valid trip-vehicle pairs construct a bipartite graph B , where each link $l = (u, v) \in B$ connects a trip $u \in U$ to a vehicle $v \in V$ with a cost weight C_{uv} , if the vehicle can feasibly serve the trip (i.e., within time constraints). C_{uv} is set to the pickup delay time δ_{uv}^{pu} in this study.

The optimization problem is to find a trip-vehicle matching solution $M \subseteq B$ that minimizes the sum of the total pickup time δ_{uv}^{pu} of all trips in each batch:

$$\min_x \sum_{(u,v) \in B} \delta_{uv}^{\text{pu}} \cdot x_{uv}$$

Subject to:

$$\sum_{v \in V} x_{uv} \leq 1, \quad \forall u \in U \quad (1)$$

$$\sum_{u \in U} x_{uv} \leq 1, \quad \forall v \in V \quad (2)$$

$$x_{uv} = 0, \quad \text{if } \delta_{uv}^{\text{queue}} > t_{\text{queue}}^{\max} \text{ or } \delta_{uv}^{\text{pu}} > t_{\text{pu}}^{\max} \quad (3)$$

$$x_{uv} \in \{0, 1\}, \quad \forall (u, v) \in B \quad (4)$$

where δ_{uv}^{pu} refers to the expected time for vehicle v to pick up trip u and x_{uv} is a binary variable indicating whether this trip-vehicle pair is selected. Constraints (1) and (2) state that each passenger and each vehicle can be matched at most once in the batch. We employed the Jonker–Volgenant (JV) algorithm [34] to solve this problem by iteratively refining a matching between trips and vehicles. It takes as input a cost matrix $C \in \mathbb{R}^{|U| \times |V|}$, where each entry C_{uv} encodes the pickup delay of assigning vehicle v to trip u , and produces as output an optimal matching $M \subseteq U \times V$ that minimizes the total cost. The algorithm maintains dual variables for trips and vehicles, constructs layered graphs to identify augmenting paths, and alternates between augmenting the current matching and adjusting the dual variables to update reduced costs. By repeating these steps until no further improvement is possible, the JV algorithm is guaranteed to obtain the theoretical optimal solution to the assignment problem.

3.3. Experimental data and settings

All experiments are carried out based on taxi operations data from street-hailing services in Chengdu, China and its road network within the Ring

Expressway. The network covers the operating area of cruising taxis [35], which is modeled as a directed graph $G = (N, E)$ with $|N| = 1\,902$ nodes and $|E| = 5\,943$ edges.

Cruising taxi operations data. We use GPS trajectories of cruising taxis in Chengdu in April, 2015 (described in Table 3). This dataset provides an unbiased view of street-hailing taxi trips because it was collected before the legalization of ride-hailing services in Chengdu in 2016. For each trip record, we use the raw record of street-hailing taxis described in Table 3. We only match trips where both their origin and destination are within 200 meters from at least one intersection node, which preserves more than 98% of the records. On selected operational days, an average of over 400,000 trips were recorded, involving more than 10,000 active vehicles. Then performances of both street-hailing and ride-hailing services can be evaluated in a fair way, given identical trips and active fleet sizes.

Table 3: Fields and Descriptions of Street-hailing Trip Data

| Field | Description |
|---------------------|--|
| Vehicle ID | Unique taxi identifier |
| Pickup location | Latitude and longitude of the trip’s start location |
| Dropoff location | Latitude and longitude of the trip’s end location |
| Pickup time | Start time of a trip |
| Dropoff time | End time of a trip |
| Deadheading mileage | Distance without passenger between consecutive trips |

Travel speed and time. To simplify the model, we assume that the routes of ride-hailing and street-hailing vehicles follow the shortest-time path to pick up and serve a trip. The corresponding road network speed is estimated us-

ing a gradient descent algorithm [36] leveraging the historical taxi trip data. Then we figure out travel time of each road segment in each hour by dividing the length of each road segment by the speed in the corresponding time period. Finally, the Floyd–Warshall algorithm [37] is employed to compute the all-pairs shortest travel time matrices across the entire network over 24 hours. All algorithms and processing details related to the estimation of driving speed and time can be found in Section 1 of Appendix. In the data preprocessing stage, certain trips are excluded to improve the reliability of the analysis. Specifically, trips with loops (where the origin and destination coincide) are removed, together with trips that are unrealistically short or excessively long. Route computation is then performed by assigning an identical initial speed $v_{\text{int}} = 40$ km/h to all road segments, following the procedure described above. Roughly 95% of the original trips remain available for further estimation. We further set the upper and lower bound of travel speeds for all road segments as $[5, 80]$ km/h based on historical speed data on the road network of Chengdu. We obtain reasonable travel times according to the following setting: Average road network speeds are highest during off-peak hours (midnight to early morning) with around 38 km/h, gradually decrease during the morning commute, and reach the lowest values during the morning (around 8:00) and evening (17:00–19:00) peak periods with around 28 km/h.

Initialization of dynamic fleet size and vehicles state. To make a fair comparison between ride-hailing and street-hailing services, we set the fleet size of ride-hailing equal to that of street-hailing. Meanwhile, we dynamically set the number of active vehicles of ride-hailing services equal to the real num-

ber of cruising taxis according to the historical data of street-hailing services. We assume that whether a vehicle is active or not is updated at the start of each hour because drivers might keep searching or waiting for additional requests after completing their last trip. Then each time period within the hour follows this setting. Let N_h^{active} denote the number of active vehicles at the start of hour h , defined as:

$$N_h^{\text{active}} = N_h^{\text{vac}} + N_h^{\text{pu}} + N_h^{\text{car}} \quad (5)$$

where N_h^{vac} , N_h^{pu} , and N_h^{car} represent the numbers of vacant, picking-up, and passenger-carrying vehicles in hour h , respectively. For hour $h + 1$, vehicle states are updated according to the following rules: (i) If $N_h^{\text{active}} < N_{h+1}^{\text{active}}$: A subset of resting vehicles ($s_v = 0$) is randomly put into the vacant state ($s_v = 1$) until the active fleet size reaches the required size; (ii) If $N_h^{\text{active}} > N_{h+1}^{\text{active}}$: vehicles are randomly deactivated in the following priority order: first, vacant vehicles are randomly put into the resting state ($s_v = 1 \rightarrow 0$); second, the picking-up vehicles are randomly set ($s_v = 2 \rightarrow 0$); finally, passenger-carrying vehicles are randomly set ($s_v = 3 \rightarrow 0$), until the active fleet size is reduced to N_{h+1}^{active} . Vehicle positions are initialized once per simulation day by randomly assigning each vehicle to the origin node of a historical trip.

All simulations and algorithm implementations are conducted using Python 3.11 and executed on a workstation with an AMD Ryzen 9 5900X CPU (3.7 GHz) and 32 GB RAM. Due to the stochasticity introduced by random initial vehicle locations each day and stochastic vehicle state transitions every hour, we performed 30 independent Monte Carlo simulations for each t_{pu}^{max} and t_{queue}^{max} to ensure the robust results.

3.4. Key performance indicators

We adopt three key performance indicators, average passenger waiting time (APWT), average deadheading mileage (ADM), and average deadheading energy consumption (ADEC), to evaluate the performance of both ride-hailing and street-hailing services. The calculation of the three key performance indicators for ride-hailing services is introduced as follows.

(i) APWT is defined as the average passenger waiting time for trips served. The waiting time for a trip u is the sum of the queuing time δ_u^{queue} before this trip is accepted and the pickup time δ_u^{pu} taken for a vehicle to arrive at the origin node of this trip, which is formulated as:

$$\text{APWT} = \frac{1}{|U_{\text{served}}|} \sum_{u \in U_{\text{served}}} (\delta_u^{\text{queue}} + \delta_u^{\text{pu}}), \quad (6)$$

where U_{served} refers to the set of served trips.

(ii) ADM refers to the average distance of all deadheading trips. A deadheading trip is defined as a trip without passengers between two consecutive service trips. The distance of a deadheading trip (denoted by md , in kilometers) is defined as the Manhattan distance between the drop-off node (d_{u-1}) of the previous trip $u-1$ to the pick-up node (o_u) of the trip u on the network G .

$$\text{ADM} = \frac{1}{|U_{\text{served}}|} \sum_{u \in U_{\text{served}}} md_{(d_{u-1}, o_u)}, \quad (7)$$

$$md_{(d_{u-1}, o_u)} = \|d_{u-1} - o_u\|_1, \quad (8)$$

(iii) ADEC is the average energy consumption of deadheading trips. We use the energy consumption formula of electric vehicles to calculate the ADEC of all deadheading trips. Let td represent the travel time (minutes). The energy consumption of each deadheading trip DEC is estimated using a macro-level model referring to the work of Raguso et al. [38]:

$$DEC(md, td) = B_1 \cdot md + B_2 \cdot \left(\frac{60 \cdot md}{td} \right)^2 \cdot md, \quad (9)$$

where B_1 and B_2 are empirically calibrated coefficients, set as 0.132 and 5×10^{-6} respectively. The ADEC (in kWh) is then formulated as:

$$\text{ADEC} = \frac{1}{|U_{\text{served}}|} \sum_{u=1}^{|U_{\text{served}}|} DEC[md_{(d_{u-1}, o_u)}, td_{(d_{u-1}, o_u)}], \quad (10)$$

The three key performance indicators of street-hailing services are calculated or obtained as follows: The APWT of street-hailing services cannot be directly observed in the street-hailing operations dataset, thus it is obtained by a 2015 travel survey conducted in major cities including Chengdu [39], which included data from hundreds of respondents. The ADM is calculated based on historical service trips of all cruising taxis in Chengdu during the study period (see Section 2 in Appendix). The ADEC is then calculated using Equations (9)-(10) based on the deadheading miles and travel time of street-hailing services.

4. Results

To make a fair comparison between the street-hailing and ride-hailing services, all trips in the street-hailing service dataset need to be served in

the simulated ride-hailing system within reasonable passenger queuing times. We thus conduct experiments to explore parameter settings for the ride-hailing system that can achieve a 100% service rate (i.e., the percentage of trips successfully served) and reasonable passenger queuing times. Figure 3 shows the changes of service rates and average passenger queuing times over different maximum queuing times $t_{\text{queue}}^{\text{max}}$ and maximum pickup times $t_{\text{pu}}^{\text{max}}$. The results illustrate that when $t_{\text{pu}}^{\text{max}} < 8$, not all trips can be served, with obviously longer queuing and picking up time for the served trips. However, when $t_{\text{pu}}^{\text{max}} \geq 8$, all trips are successfully served, and the average passenger queuing time of the ride-hailing system drops rapidly to a very low level (≈ 1 minute). We therefore set $t_{\text{pu}}^{\text{max}} \geq 8$ minutes to guarantee a service rate of 100%. Following this setting, the average passenger queuing time remains nearly constant for $t_{\text{queue}}^{\text{max}} \geq 10$ and we thus simply set $t_{\text{queue}}^{\text{max}} = 20$ minutes.

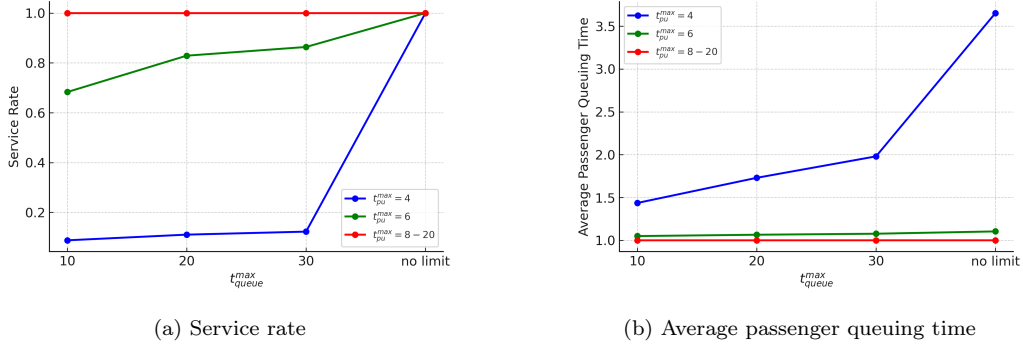


Figure 3: Service rate and average passenger queuing time of ride-hailing services influenced by $t_{\text{queue}}^{\text{max}}$ and $t_{\text{pu}}^{\text{max}}$

4.1. Comparison between ride-hailing and street-hailing Services

We compare three key performance indicators of street-hailing services with those of ride-hailing services under different settings of maximum pas-

senger pickup time t_{pu}^{\max} representing the service radius of vehicles.

First, we examine the effect of t_{pu}^{\max} on the performances of ride-hailing services for all service trips in the study period. Results in Figure 4 show that t_{pu}^{\max} is a crucial operational parameter in centrally dispatched ride-hailing services and has a substantial impact on the overall system efficiency. Increasing t_{pu}^{\max} leads to obvious improvements in all three performance indicators. Specifically, APWT decreases from 2.32 min at $t_{pu}^{\max} = 8$ min to 2.27 min at $t_{pu}^{\max} = 18$ min, ADM decreases from 0.64 km to 0.62 km, and ADEC decreases from 0.095 kWh to 0.092 kWh. Notably, although these correlations between t_{pu}^{\max} and three key performance indicators are statistically significant and consistent when $t_{pu}^{\max} \leq 14$ minutes, they become not significant as t_{pu}^{\max} further increases, also shown in Figure 4 with a 95% confidence intervals.

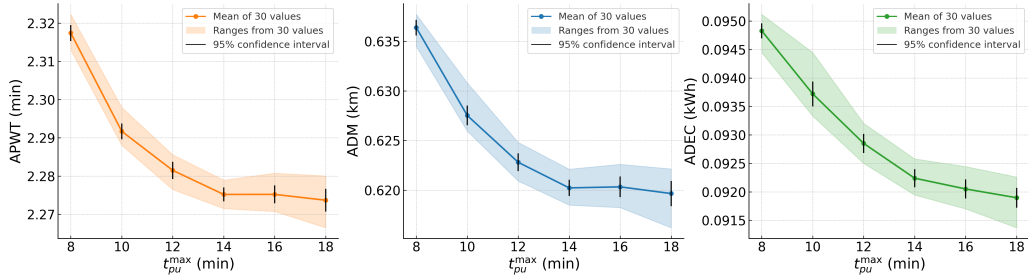


Figure 4: Changes of ride-hailing performances over the maximum pick-up time t_{pu}^{\max} . Average passenger waiting time (APWT), average deadheading mileage (ADM), and average deadheading energy consumption (ADEC) all decrease as t_{pu}^{\max} increases, while these improvements gradually diminish. The light-colored bands represent the range of results from all 30 random experiments. Each data point represents the mean value derived from the corresponding experiments, with vertical error bars indicating the 95% confidence intervals.

Figure 5 further demonstrates that ride-hailing services at $t_{pu}^{\max} \in [8, 20]$ perform much better than street-hailing on all three key performance in-

dicators. In terms of APWT, the ride-hailing system can achieve an 81% improvement when $t_{pu}^{\max} \geq 8$ compared to street-hailing. It also shows that over 99.9% trips can be matched by the platform within 1 minute, indicating that the ride-hailing system achieves a high operational efficiency with batch matching. Figure 6 shows that the APWT distribution of street-hailing services is more dispersed and a large proportion of trips require longer waiting times, compared to that of ride-hailing services. A majority of ride-hailing trips are responded to and picked up within 5 minutes, while 39% of street-hailing trips need a 10–15 minute waiting time and 20% take longer than 15 minutes. This indicates that street-hailing services tend to require more time to fulfill a trip request, suggesting lower system efficiency and greater variability in passenger queuing time. As for ADM and ADEC, ride-hailing services also show consistently better performance than street-hailing services when $t_{pu}^{\max} \geq 8$, with a 75% and 72.1% improvement respectively.

4.2. Spatiotemporal analysis of ride-hailing services

We further conduct a spatiotemporal analysis with $t_{pu}^{\max} = 16$ and $t_{queue}^{\max} = 20$ to understand how the ride-hailing performance varies throughout the day and across city areas. We set t_{pu}^{\max} to 16 minutes because further increasing t_{pu}^{\max} does not bring obvious changes on the 3 key performance indicators (As shown in Figure 4).

Temporal analysis. Figure 7 shows the hourly variation of the ride-hailing fleet size in different states over a 72-hour operational period. The utilization of the vehicles remains relatively stable throughout the day, with around 60% of the active vehicles (the black line) being with passengers (the blue line),

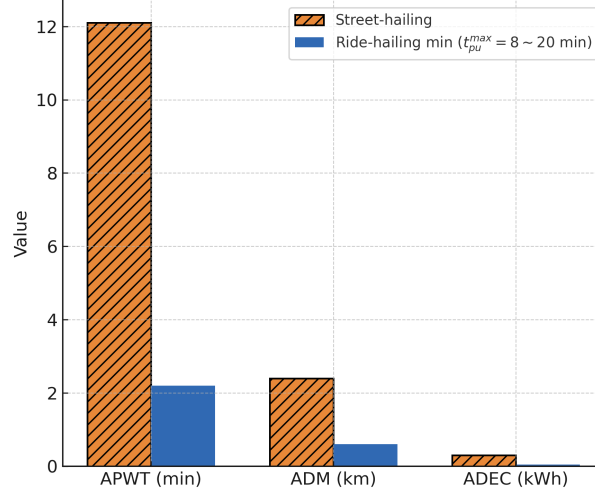


Figure 5: Comparison between ride-hailing (at $t_{pu}^{max} \in [8, 20]$ minutes) and street-hailing services. The performances of ride-hailing service with $t_{pu}^{max} \in [8, 20]$ have no noticeable difference.

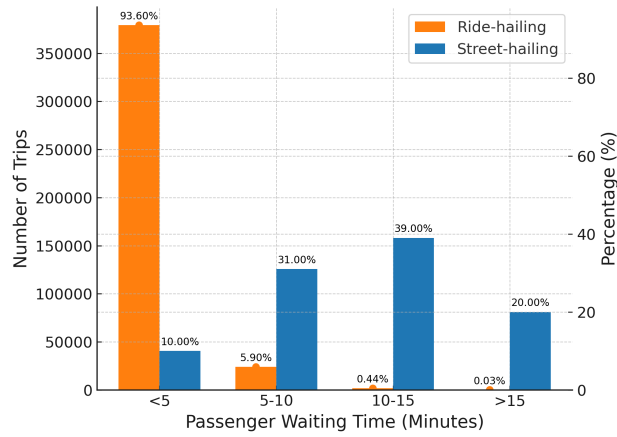


Figure 6: Effects of passenger waiting time on the number of trips served in the ride-hailing and street-hailing systems.

despite significant fluctuations in the total number of trips (the red line).

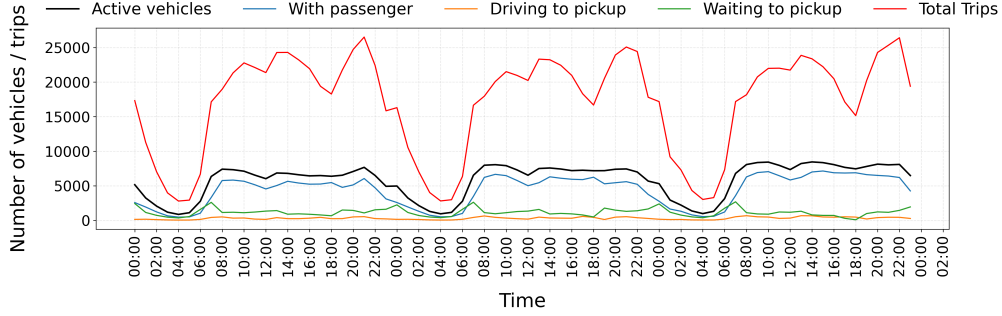


Figure 7: Changes of the number of vehicles in different states over time.

Figure 8 shows the hourly waiting time for ride-hailing and street-hailing services. In terms of APWT, the two services exhibit similar trends, with ride-hailing consistently demonstrating superior performance. Specifically, the APWT exceeds 8 minutes during the morning rush hour (i.e., 8-9 a.m.). This peak coincides with an increase in both queuing time and pickup time, which is caused by a surge in demand that overwhelms the available service capacity within a short time window. Considering the trend throughout the entire day, as the queuing time stays at a low level, the variation in APWT is primarily driven by fluctuations in the pickup time. Overall, ride-hailing services outperform street-hailing on APWT throughout the day because the online platform enables better matchings.

Figure 9 presents the ADM comparison of the two services. The ADM in the ride-hailing system remains relatively stable over time, with vehicles traveling distance approximately from 0.45 to 1.20 km on average to pick up passengers in each hour. This value is substantially lower than the ADM observed in street-hailing services throughout the entire day. The ADM of

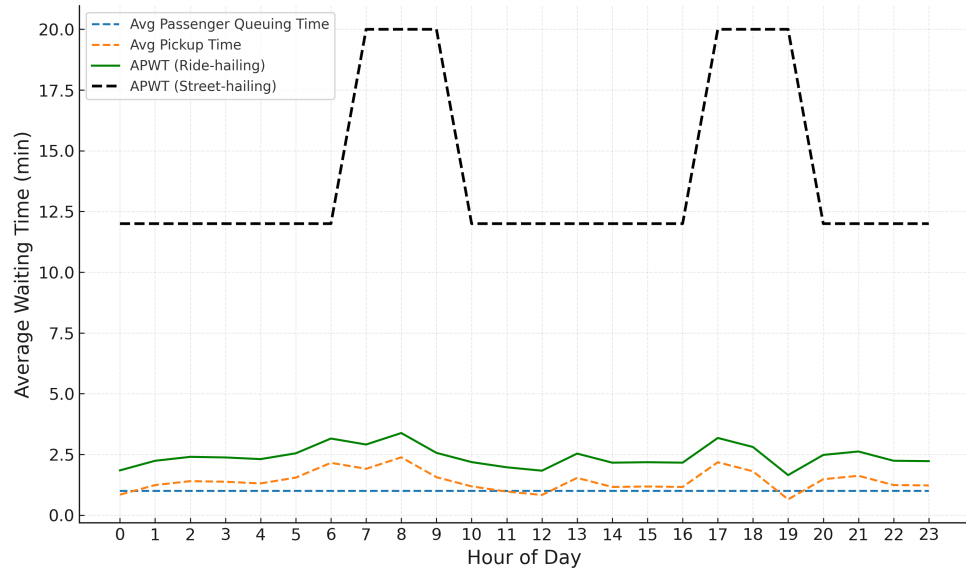


Figure 8: Comparison of average waiting times in the ride-hailing and street-hailing systems.

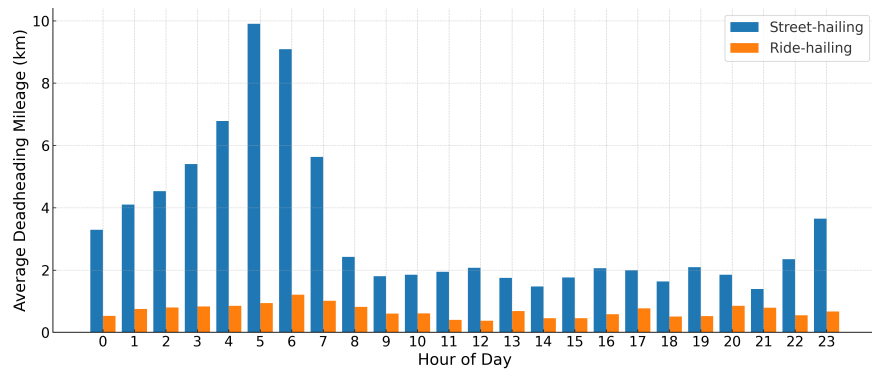


Figure 9: Comparison of ADM in the ride-hailing and street-hailing systems.

street-hailing services varies significantly over time. During high-demand periods, such as in daytime and early evening, street-hailing drivers only travel about 1.5–3 km to pick up their next passenger. It indicates that the ride-hailing system becomes particularly advantageous under low-demand conditions, compared to street-hailing services, because ride-hailing services can directly assign vehicles to passengers, eliminating the large amount of random cruising in street-hailing services when trip requests are scarce. In addition, although there is a large difference in ADM values between street-hailing and ride-hailing services, the variation of ADM in both hailing systems share a similar pattern: periods of high ADM for street hailing also correspond to high ADM for ride hailing: Street-hailing exhibits a pronounced peak in ADM between 4:00 and 6:00 a.m., while ride-hailing shows an obvious increase during the same period; Both systems maintain relatively low ADM values during daytime hours, followed by a moderate rise late at night. This indicates that the substantial differences in ADM values are mainly caused by different hailing service modes, while the resemblance in their variation patterns may result from shared characteristics, such as demand pattern, road network topology, and real-time traffic speeds.

Spatial analysis. To further explore the spatial heterogeneity of service performance, we divide the experimental region of Chengdu into three zones, as shown in Figure 10. The area within and along the Second Ring Road is defined as the city center; the area outside the Second Ring, excluding the neighborhood of Shuangliu International Airport, is defined as the outer region; and the area surrounding the airport is treated as a distinct zone (i.e., airport area). This division is also consistent with the actual situation

in Chengdu. We analyse all trips originating from these zones between 07:00 and 23:00, which covers the primary operational hours of on-demand travel operations.

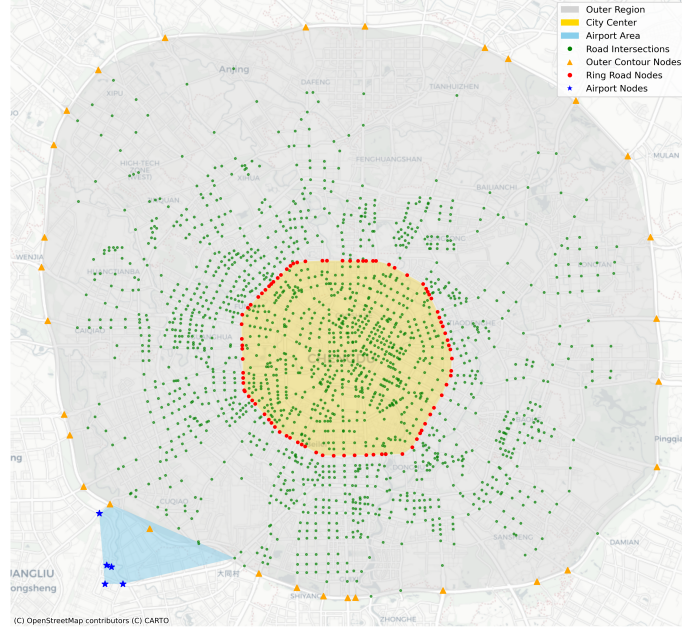


Figure 10: An illustration of the Chengdu map divided into three functional zones: Outer Region, City Center, and Airport Area. Road intersections and boundary nodes are marked.

Figure 11 shows the comparison of ADM in different zones for ride-hailing and street-hailing services. Overall, ride-hailing services perform better than street-hailing in every zone. Specifically, street-hailing taxis cruise for 1.47 km to pick up a passenger in city center on average, while ride-hailing vehicles travel 0.54 km. In the outer region, the ADM of street-hailing and ride-hailing services are 2.85 km and 0.72 km, respectively. Notably, in the airport area, the ADM is 4.82 km for street-hailing services but only 0.09 km for ride-hailing, showing the largest difference among the three areas. It is be-

cause street-hailing taxi drivers often head to airports to pick up passengers intentionally, as such trips are typically longer in mileages and yield higher fares. In contrast, ride-hailing drivers cannot freely select their trips. They usually arrive in the airport area because they receive trips directed there. Owing to the relative scarcity of trips in the vicinity, ride-hailing drivers tend to remain in the airport area for extended periods. Consequently, when a new demand arises, they are able to pick up the passenger with a short deadheading distance.

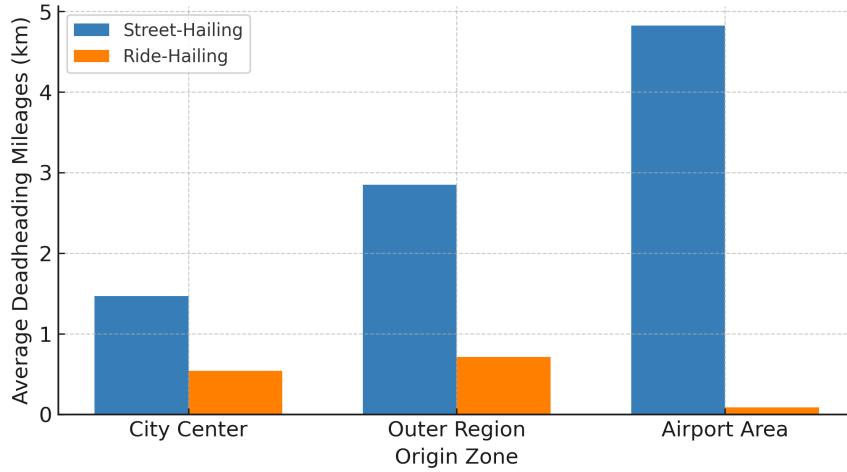


Figure 11: Comparison of ADM in different zones for ride-hailing and street-hailing services.

In summary, by the comparison of the ride-hailing and street-hailing services presented in Section 4.1, we can conclude that, with a properly configured matching mechanism, the ride-hailing system consistently maintains a high service rate with a lower APWT, ADM and ADEC compared with those of street-hailing services. By the spatiotemporal analysis of ride-hailing services, we found that this advantage persists across all spatiotemporal con-

ditions we considered, and intensifies under sparse demand, such as during late-night hours or airports vicinities.

5. Discussion on ride-hailing service Policies

A range of policy interventions have been reported to improve the performance of ride-hailing services. We further discuss the effects of three representative policies, fleet size management, geofencing and demand management policy.

5.1. Fleet size management

To evaluate how the ride-hailing fleet size influences its service performance and traffic conditions, we conduct a controlled experiment in which the baseline fleet size is multiplied by a scaling factor F , ranging from 0.8 to 2.0 with a step size of 0.1, which simulates scenarios of fleet size reduction and expansion. Given that ride-hailing vehicles constitute a significant portion of urban traffic, changes in fleet size may affect road congestion and travel speed. Specifically, a larger fleet size exacerbates the urban congestion due to additional travel and curbside parking pressure, leading to a lower network speed. We follow the method introduced by Beojone et al. [27], and adopt a simplified macroscopic fundamental diagram (MFD) to simulate road network speeds under different fleet sizes (see Section 3 in Appendix).

Simulation results (Figure 12) show that reducing fleet size leads to larger APWT, ADM and ADEC when $F \in [0.9, 1.0)$. When the fleet size is reduced to 80% of the baseline size, the APWT further rises and the fleet fails to serve all trips. On average, an additional 10% increase in fleet size when $F \in [0.9, 2.0]$ yields less than a 2% reduction in APWT and a 5% reduction

in both ADM and ADEC. This indicates that when vehicles are allowed to park on roadsides after completing their trips, the bottlenecks in ride-hailing services is not only insufficient supply: merely increasing fleet size brings limited and diminishing benefits.

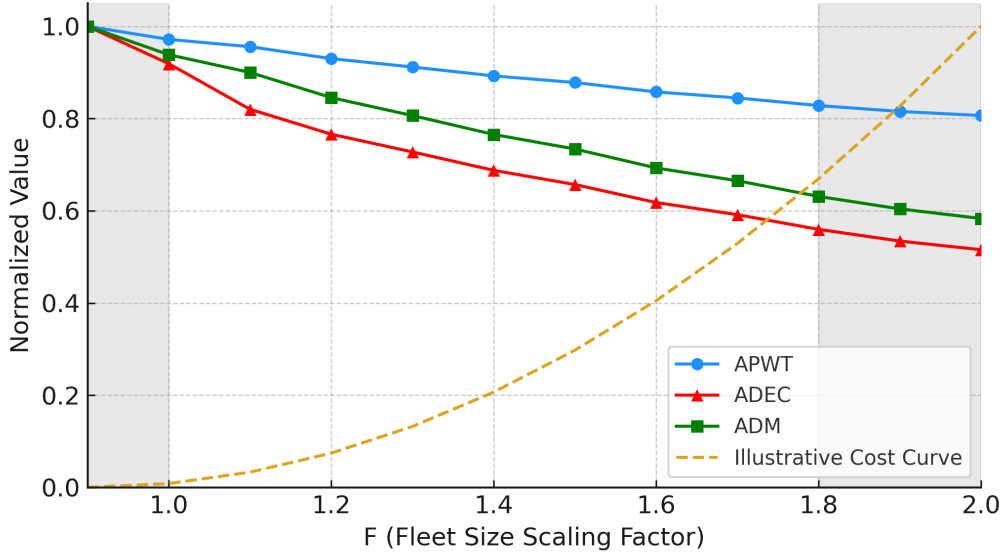


Figure 12: Normalized trends of APWT, ADM, and ADEC under different scaling factors of fleet size. The cost curve indicates that as the fleet size increases, its marginal cost gradually rises [40]. The recommended fleet size range is illustrated by the values $F = 1.0$ to $F = 1.8$. When $F > 1.8$, all three indicators (APWT, ADM, and ADEC) show diminishing marginal improvements as the fleet size increases.

5.2. Geofencing

As shown in Figure 11, more deadheading occurs in the outer region of the city, whereas vehicles operating in the city center exhibit higher utilization efficiency. Some cities have restricted ride-hailing services in specific areas such as airports or city centers, or have required vehicles to operate only within their registered administrative regions, which is also called a ge-

ofencing policy [41, 42]. We thus investigate the effect of geofencing policy on the performance of ride-hailing services.

Following Section 4.2, we divide Chengdu into two operational zones using the Second Ring Road as a geographic boundary: the city center and the outer region. This division also aligns with traffic restriction policies implemented in some megacities like Shanghai, China, where certain vehicles are not permitted to enter the city center. Our geofencing policy considers three independent operators (Operators 1-3) operating in different regions respectively, as shown in Figure 13. Operator 1 serves trips whose origin and destination are both within the city center, Operator 2 serves trips within the outer region. Operator 3 serves cross-zone trips that span these two regions. Each operator has a separate fleet and provides ride-hailing services using its dedicated platform. According to the historical trip data, trips of the three operators account for approximately 37.5%, 25%, and 37.5% of the total number of trips in Chengdu, respectively. We first consider a basic geofencing policy that allocates the fleet to the three operators proportionally based on the share of their trips in the total number of trips, with the same t_{pu}^{\max} for all operators.

We find that the geofencing slightly reduces the service capacity of the ride-hailing system: with the original fleet size, Operator 2 and Operator 3 fails to serve approximately 0.5% of the trips, mainly due to a sparser distribution of trips in the outer region and cross-region and the resulting longer passenger waiting and service time. Overall, we observe a 15% deterioration on APWT, alongside deterioration of 28.6% on ADM and 34.5% on ADEC compared to the performance of the ride-hailing system without implement-

ing the geofencing policy. Dividing trips by operators according to their origin-destination locations in ride-hailing services results in a deterioration of the overall system performance, which is consistent with the findings of previous studies on multi-operator settings [23].

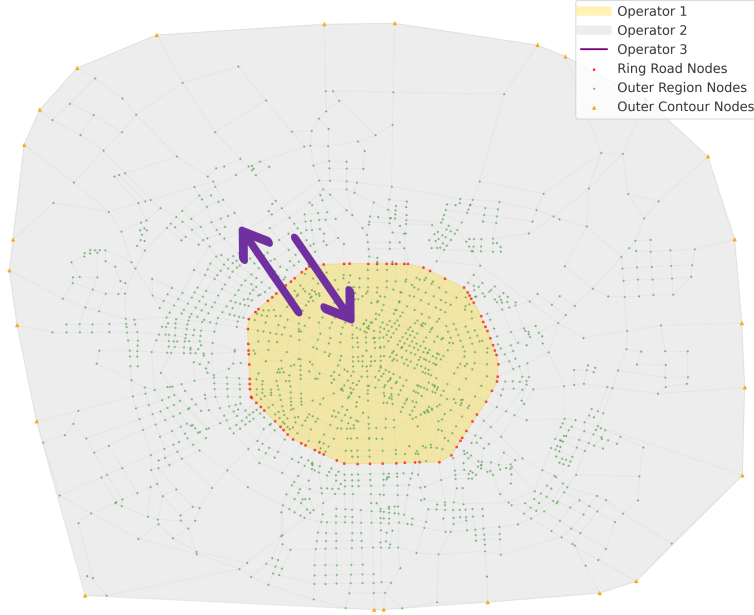


Figure 13: Service area division for Operator 1-3 in Chengdu: Operator 1 covers the city center (within the Second Ring road), Operator 2 covers the outer region, and Operator 3 serves passengers travel across two regions.

However, this does not imply that the geofencing policy is completely inefficient. Under the geofencing policy, ride-hailing performs significantly better when serving trips within the city center (accounting for approximately 37.5% of daily trips). Specifically, APWT, ADM, and ADEC were improved substantially by 23%, 44.7%, and 43.9%, respectively. In addition, Operator 1 outperforms the other two operators in terms of APWT, ADM, and ADEC, and further demonstrates low vehicle utilization. In contrast, Operators 2

and 3 exhibit a certain degree of inefficiency due to more dispersed trips and longer average trip mileages.

In light of these results, we conduct an extended experiment in which we reduce the $t_{\text{queue}}^{\text{max}}$ for Operator 1 from 16 minutes to 12 minutes and increase the fleet sizes of Operators 2 and 3 by 500 vehicles, respectively, reallocated from the fleet of Operator 1. We compare this fine-tuned geofencing policy with the basic one. The results show that the fine-tuned geofencing system achieves significant improvements on APWT (3.5%), ADM (6.6%) and ADEC (10.6%) compared to the basic geofencing system, as shown in the Figure 14.

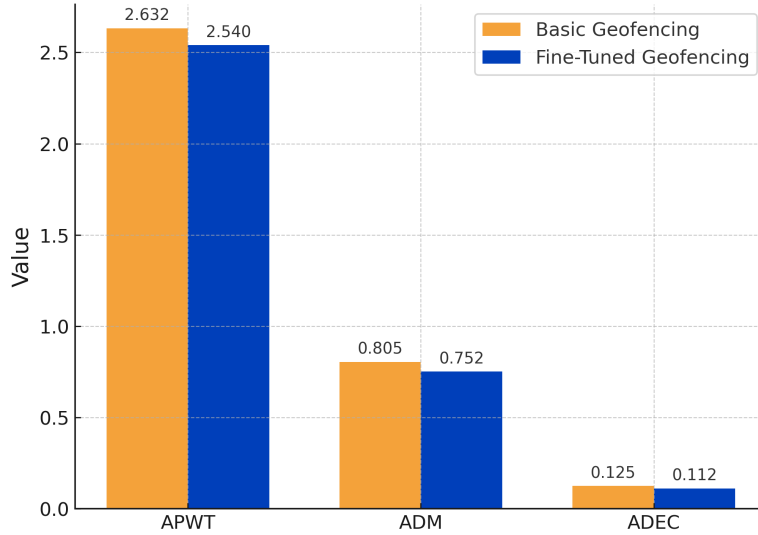


Figure 14: Performance comparison between basic and fine-tuned geofencing settings in terms of the three key performance indicators.

Overall, our results show that a geofencing policy leads to worse performance on APWT, ADM and ADEC, which is consistent with the result found by Vazifteh et al [23] (i.e., multi-operator performs worse than single

one). Meanwhile, the performance for serving trips within the city center improves significantly with the geofencing policy that treats the city center and other areas as distinct and independent operating zones. Moreover, compared to the basic geofencing setting, the fine-tuned geofencing setting with more appropriate allocated fleet sizes and clearly geographic service responsibilities, can facilitate better performance on all the three key performance indicators. This fine-tuning problem can be solved as a fleet/resource allocating problem to achieve better overall performance.

5.3. Demand management

We further evaluate whether and how demand management policy impacts the performance of ride-hailing services. Some ride-hailing platforms implement demand management by rejecting or assigning certain requests with lower priority, or by indirectly stimulating or suppressing demand through such mechanisms as dynamic pricing. Next, we discuss which types of demand should be managed and how demand management affects the performance of ride-hailing services. The amount of system resources required by a trip is determined by its spatiotemporal characteristics, including the origin and destination locations and the departure time [43]. As the effect of rejecting a single trip is too small to be evaluated, we design a scenario-based experiment that removes a set of trips with particular spatiotemporal features, and then evaluate the resulting changes in system performances through controlled simulations.

For temporal characteristics, each day is divided into **peak** and **offpeak** periods, representing hours with higher or lower travel demand, respectively. For spatial characteristics, we use two labels (i.e., x and y) to represent the

spatial characteristics of each node in the graph G , which measure whether the node is high-demand and high-attraction. If the number of trips starting from a node is large, this node is called a high-demand node and we set $x = 1$; otherwise, it is a low-demand node and we set $x = 0$. Similarly, if the number of trips ending at a node is large, this node is called a high-attraction node and we set $y = 1$; otherwise, it is low-attraction and we set $y = 0$. Let $O_{xy}D_{xy}$ denotes the spatial characteristics of a trip from its origin O to the destination D . For example, $O_{11}D_{00}$ means that the trip's origin is high-demand and high-attraction, while the destination is low-demand and low-attraction. High-demand and high-attraction nodes are identified using a statistical outlier detection method based on Z-scores of trip origins and destinations (see Appendix Section 4).

We then conduct a sensitivity analysis based on the spatial and temporal characteristics. A total of 18 scenarios are developed. Each scenario is formed by randomly deleting 2,000 trips with a specific label (e.g., high-demand, low-attraction). Two of these scenarios delete trips started during peak or offpeak hours. The other sixteen (2^4) of these scenarios delete trips according to spatial characteristics (i.e, whether the origins and destinations of trips are high-demand/high-attraction or not). However, six scenarios are not analysed because the number of trips in each of these scenarios is less than 2,000. We also consider a baseline scenario **random**, in which 2,000 trips are randomly deleted. To ensure the robustness of the results, each scenario is independently simulated 30 times by randomly deleting trips.

Overall, no significant difference is observed in terms of ADM and ADEC across all scenarios deleting trips with any spatial or temporal characteristic

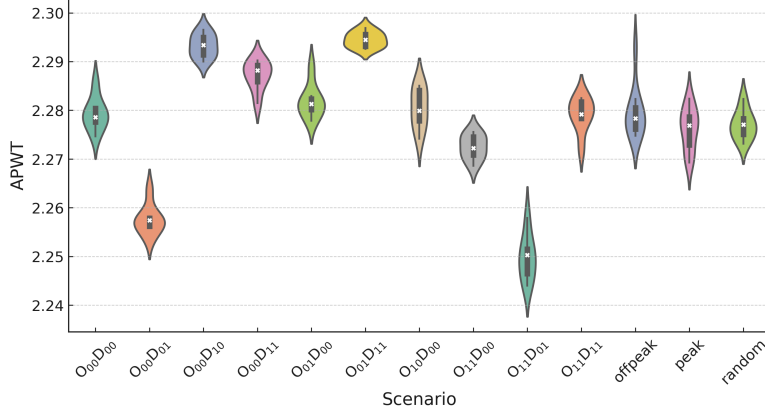


Figure 16: Distribution of APWT in 13 scenarios. The white dot in each violin represents the median of the distribution.

6. Conclusion

This study presented a simulation framework to evaluate the performance of ride-hailing services and made a fair comparison for ride-hailing and traditional street-hailing services in terms of three key performance indicators, namely average passenger waiting time (APWT), average deadheading miles (ADM) and average deadheading energy consumption (ADEC), based on a real street-hailing taxi operations dataset. We considered key real-world characteristics of on-demand mobility systems, including real-time trip-vehicle matching, maximum passenger queuing time, and maximum pickup time. Our results revealed that compared to the street-hailing service, the ride-hailing service can effectively reduce the APWT, ADM and ADEC by 81%, 75%, 72.1%, respectively. In particular, the ride-hailing service exhibits greater performance improvements during mid-night low-demand periods and in remote areas such as airports, compared with other spatiotemporal conditions.

We evaluated the impacts of three types of policy interventions from both supply- and demand-side perspectives on the performance of ride-hailing services. From the supply side, increasing fleet size exhibits gradually converging improvements, suggesting that the marginal benefits decrease as the fleet expands. Meanwhile, the geofencing policy leads to worse overall performance, but significantly better performance for serving trips within the city center. Moreover, simultaneously allocating regional fleet size and adjusting region-specific dispatch parameters (i.e., t_{pu}^{\max}) generates better performances than applying geofencing policies alone on the three performance indicators. On the demand side, we found that rejecting trips destined for nodes that are high-attraction but not high-demand could substantially reduce the APWT without negatively affecting the ADM and the ADEC.

This study was conducted based on the assumptions that the platform fully determines vehicle-trip matching and that vehicles wait in place after each trip, which closely simulate the settings of autonomous mobility on-demand (AMoD) services. Thus, our approach offers a valuable benchmark for evaluating AMoD service performance, and our findings can be used as a reference for the design of efficient AMoD systems. Our results also suggested that providing high-quality, resource-efficient ride-hailing services requires not only algorithmic optimization, but also targeted policy interventions that enhance spatial coordination and smooth temporal demand fluctuations. Future research could incorporate more realistic behavioral modeling, dynamic pricing mechanisms, or explore multi-modal coordination with public transit and ride-splitting services to further improve system sustainability. It is also important to take repositioning strategies into consideration to mitigate the

supply–demand imbalance in ride-hailing services.

7. CRediT authorship contribution statement

Youkai Wu: Writing - original draft & editing, Methodology, Investigation, Validation. **Zhaoxia Guo:** Conceptualization, Data curation, Resources, Project administration, Writing – review & editing. **Qi Liu:** Writing - original draft, review & editing, Data curation, Resources, Project administration. **Stein W. Wallace:** Writing – review & editing.

8. Data availability

Data and all codes are available at: <https://github.com/youkaiwujasper/ride-hailing-dispatch>.

9. Acknowledgements

This research was funded by the National Natural Science Foundation of China (72171159, 72361137004, and 72404200), and the China Postdoctoral Science Foundation (GZC20241170).

Appendix A. Estimation of the travel time on the road network

We utilize a gradient descent algorithm leveraging taxi trip records to estimate the time-dependent average travel time of each road segment. Based on these edge-level travel times, the Floyd–Warshall algorithm is then employed to compute the all-pairs shortest travel time matrices across the entire network, thereby capturing the spatiotemporal accessibility dynamics over 24 hours. The procedure for training the model is shown in Algorithm 1.

Algorithm 1 From Trip Records to Hourly All-Pairs Travel Time Matrices

```

1: Input: Directed road network  $G = (N, E)$  with edge lengths  $\ell_e$ ; trip
   dataset  $\mathcal{T} = \{(n_o, n_d, H, T^{obs})\}$ 
2: Output: Hourly all-pairs shortest travel time matrices  $\{D^H\}_{H=0}^{23}$ 
3: for each hour  $H \in \{0, \dots, 23\}$  do
4:   Step 1: Estimate edge travel times via gradient descent
5:   Extract trips  $\mathcal{T}_H = \{(n_o, n_d, T^{obs}) \mid (n_o, n_d, H, T^{obs}) \in \mathcal{T}\}$ 
6:   Initialize edge times  $t_e^H \leftarrow \frac{\ell_e}{v_0}$ ,  $v_0 = 20$  km/h,  $\forall e \in E$ 
7:   repeat
8:     Set gradients  $g_e \leftarrow 0$ ,  $\forall e \in E$ 
9:     for each trip  $(n_o, n_d, T^{obs}) \in \mathcal{T}_H$  do
10:      Compute shortest path  $P(n_o, n_d)$  in  $G$ 
11:      Predict travel time  $\hat{T} = \sum_{e \in P(n_o, n_d)} t_e^H$ 
12:      for each  $e \in P(n_o, n_d)$  do
13:         $g_e \leftarrow g_e + 2(\hat{T} - T^{obs})$ 
14:      end for
15:    end for
16:    Update edge times:  $t_e^H \leftarrow \max\{t_e^H - \eta g_e, \epsilon\}$ ,  $\forall e$ 
17:  until loss convergence
18:  Step 2: Compute all-pairs travel times via Floyd–Warshall
19:  Initialize  $D^H[i, j] \leftarrow \begin{cases} 0 & i = j \\ t_{(i,j)}^H & (i, j) \in E \\ \infty & \text{otherwise} \end{cases}$ 
20:  for  $k \in N$  do
21:    for  $i \in N$  do
22:      for  $j \in N$  do
23:         $D^H[i, j] \leftarrow \min\{D^H[i, j], D^H[i, k] + D^H[k, j]\}$ 
24:      end for
25:    end for
26:  end for
27: end for

```

Table A.4: Notation used in Algorithm 1

| Notation | Definition |
|--------------------------|---|
| $G = (N, E)$ | Directed road network with node set N and edge set E |
| $ N $ | Number of nodes in the network |
| $ E $ | Number of edges in the network |
| $e = (i, j) \in E$ | Directed edge from node i to node j |
| ℓ_e | Physical length of edge e |
| \mathcal{T} | Set of all observed trips |
| (n_o, n_d, H, T^{obs}) | A trip with origin n_o , destination n_d , hour H , observed time T^{obs} |
| \mathcal{T}_H | Subset of trips starting in hour H |
| t_e^H | Estimated travel time of edge e during hour H |
| \hat{T} | Predicted travel time of a trip (sum of edge times) |
| g_e | Gradient of loss function w.r.t. edge e |
| η | Learning rate in gradient descent |
| ϵ | Lower bound to ensure nonnegative edge times |
| $D^H[i, j]$ | Shortest travel time from node i to j during hour H |

Figure A.17 illustrates the daily variation of average travel speed across the road network. The results clearly capture typical urban traffic dynamics: speeds are highest during off-peak hours (midnight to early morning), gradually decrease during the morning commute, and reach the lowest values during the morning (around 8:00) and evening (17:00–19:00) peak periods. The recovery of speeds in late evening further confirms the method’s ability to reflect temporal fluctuations in network-wide traffic conditions.

Appendix B. ADM estimation of street-hailing services

The average deadheading miles (ADM) of street-hailing services is estimated based on its real GPS trajectory data. We use real-world GPS trajectory data from street-hailing services in Chengdu, China. Each record corresponds to a single GPS point and includes vehicle operational and po-

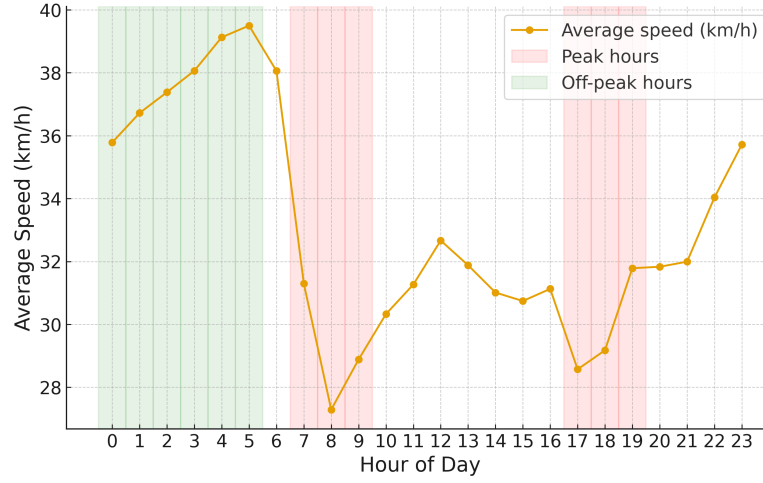


Figure A.17: Hourly variation of average travel speed across the road network.

sitional information. Key fields of the GPS data are shown in Table B.5.

Table B.5: Fields of street-hailing GPS Data

| Field | Description |
|------------|--|
| vehicle_id | Unique identifier for the vehicle |
| timestamp | GPS recorded time |
| longitude | Longitude of the vehicle location |
| latitude | Latitude of the vehicle location |
| status | Operational status of the vehicle: deadheading or occupied |

To estimate the ADM of street-hailing services, we need to identify valid deadheading trajectory segments for each vehicle and compute their travel time and distance, while excluding segments with missing or discontinuous GPS data. The notation and process are described in Table B.6 and Algorithm 2:

Based on the above algorithm, we obtain the daily deadheading travel time and mileage for each vehicle. The ADM of street-hailing services is then

Algorithm 2 Deadheading Travel Time and Distances estimation from Continuous GPS Trajectories

```

1: Input: GPS records with (vehicle_id, timestamp, latitude, longitude, status)
2: Output: Daily deadheading travel time and mileages of each vehicle
3: Sort all GPS records by vehicle_id and timestamp
4: for each vehicle do
5:   Initialize list of valid deadheading segments as  $\mathcal{S} \leftarrow \emptyset$ 
6:   Initialize empty buffer segment  $\leftarrow []$ 
7:   for each GPS record  $(t, \phi, \lambda, s)$  do
8:     if  $s = \text{deadheading}$  then
9:       Append point to segment
10:    else
11:      if segment is not empty then
12:        Append segment to  $\mathcal{S}$  and reset segment  $\leftarrow []$ 
13:      end if
14:    end if
15:  end for
16:  if segment is not empty then
17:    Append final segment to  $\mathcal{S}$ 
18:  end if
19:  Initialize deadheading_time_min  $\leftarrow 0$ ,
  deadheading_distance_km  $\leftarrow 0$ 
20:  for each segment  $s \in \mathcal{S}$  do
21:    if any time gap in  $s$  exceeds 300 seconds then
22:      continue
23:    end if
24:    Let  $t_{\text{start}}, t_{\text{end}}$  be the first and last timestamps in  $s$ 
25:     $\Delta t \leftarrow (t_{\text{end}} - t_{\text{start}})$ 
26:    Initialize  $d \leftarrow 0$ 
27:    for each consecutive point pair  $(\phi_1, \lambda_1)$  and  $(\phi_2, \lambda_2)$  in  $s$  do
28:      Compute Haversine distance  $d_{12}$  between the points
29:       $d \leftarrow d + d_{12}$ 
30:    end for
31:    deadheading_time_min  $\leftarrow \text{deadheading\_time\_min} + \Delta t$ 
32:    deadheading_distance_km  $\leftarrow \text{deadheading\_distance\_km} + d$ 
33:  end for
34:  Record (vehicle_id, date, deadheading_time_min, deadheading_distance_km)
35: end for

```

Table B.6: Notation in estimating the Deadheading Travel Time and Distances

| Symbol | Description |
|--------------------|---|
| t | Recorded time of the GPS point in the trajectory. |
| ϕ | Latitude of the GPS point (in radians). |
| λ | Longitude of the GPS point (in radians). |
| s | Vehicle status at the GPS point (e.g., deadheading). |
| t_{start} | Recorded time of the first GPS point in a deadheading segment. |
| t_{end} | Recorded time of the last GPS point in a deadheading segment. |
| Δt | Deadheading travel time of a segment, computed as $t_{\text{end}} - t_{\text{start}}$ (in minutes). |
| d_{12} | Haversine distance between two consecutive GPS points (in kilometers). |
| d | Sum of all d_{12} values within a vacant segment (in kilometers). |

computed by summing the total deadheading mileages across all vehicles and dividing it by the total number of trips.

Appendix C. Simulating road network speeds under different fleet sizes based on the macroscopic fundamental diagram model

The average travel speed on the road network is computed based on the total travel time and mileage by the macroscopic fundamental diagram (MFD) model. We construct the data points of MFD by aggregating vehicle operation records every 30 minutes across four consecutive days. For each 30-minute, we compute the total number of active vehicles in the street-hailing system and assume that street-hailing vehicles account for 10% of total vehicles on the road network. v and n represent the average road network speed and the number of vehicles running on the road, respectively. The aggregated data points (n, v) are then used to fit multiple candidate functional forms for estimating speeds $v(n)$, including linear, exponential decay, power law, and

log-shift models (Algorithm 3).

Algorithm 3 Macroscopic Fundamental Diagram (MFD) Regression Procedure

- 1: **Input:** Vehicle trip records from multiple days
 - 2: **Output:** Regression parameters for $v(n)$
 - 3: Assign each record to a 30-minute time interval t
 - 4: **for** each interval t **do**
 - 5: Compute active taxi count n_t^{taxi}
 - 6: Estimate total vehicle count $n_t \leftarrow n_t^{\text{taxi}}/0.1$
 - 7: Compute total travel time and mileage
 - 8: Calculate average speed v_t (km/h)
 - 9: **end for**
 - 10: Construct MFD points: $\mathcal{P} = \{(n_t, v_t)\}$
 - 11: **for** each candidate model $f \in \{\text{linear, exponential, power, log-shift}\}$ **do**
 - 12: Estimate parameters θ_f via non-linear regression
 - 13: **end for**
-

We evaluate each functional form using the coefficient of determination (R^2). Among all candidate functions, the exponential and log-shift models yield fitted curves that are nearly linear. We select the linear model due to its sufficient predictive accuracy ($R^2 = 0.61$) and simplicity, as shown in Table C.7 and Figure C.18. The linear model is used to estimate the average travel speed.

Table C.7: Performance of Candidate MFD Models

| Model | Parameters | R^2 |
|-------------|---|--------|
| Linear | $A = 36.998, B = -0.000202$ | 0.61 |
| Exponential | $a = 69.868, b = 3 \times 10^{-6}, c = -32.403$ | 0.61 |
| Power law | $a = 52429.814, b = 0.000, c = -52329.194$ | 0.5708 |
| Log-shift | $a = 1063.048, b = 80.264, c = 354669.766$ | 0.61 |

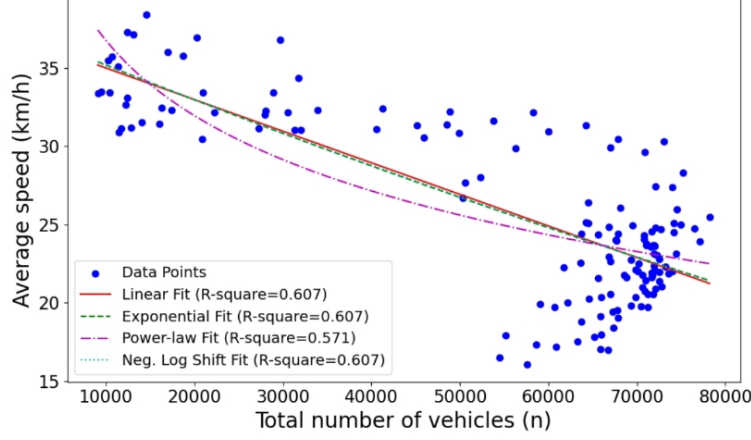


Figure C.18: Comparison of model fittings for MFD. The scatter points represent the aggregated data over 30-minute intervals. Four candidate models are tested: linear, exponential, power-law, and shifted logarithmic functions.

Appendix D. Identification of high-demand and high-attractive nodes

To analyze spatial disparities in trips demand, we classify intersections on the road network by two characteristics: demand and attractiveness. If the number of trip origins at an intersection (node) is statistically significantly higher than that at other intersections, this intersection is defined as a **high-demand node**; otherwise, it is a non high-demand node. If the number of trip destinations at an intersection node is statistically significantly higher than that at other intersections, this intersection is defined as a **high-attractive node**; otherwise, it is a non high-attractive node.

We use a statistical outlier detection method (Algorithm 4) based on the log-transformed origin and destination counts. A node is considered significantly high-demand/high-attractive if its Z-score exceeds a predefined threshold $z_{\text{threshold}}$. This approach ensures that only nodes with demand/attractiveness far exceeding the average can be classified as high-demand/high-attractive.

We set $z_{\text{threshold}} = 1.2816$, which corresponds to the 90% quantile in a one-tailed Z-test ($\alpha = 0.10$), marking the number of trips at a node as statistically significantly higher than the average origin or destination counts of all nodes.

Algorithm 4 Identification of High-Demand and High-Attractive Nodes

```

1: Input: Origin (pickup) counts  $\text{on\_count}(n)$  and destination (drop-off)
   counts  $\text{off\_count}(n)$  for all nodes  $n \in \mathcal{N}$ 
2: Output: Node  $\text{is\_high\_demand}(n)$  and  $\text{is\_high\_attractive}(n)$  for all
    $n$ 

3: Compute Z-scores of log-transformed pickup counts:  $z_n^{\text{on}} \leftarrow$ 
    $\text{Zscore}(\log(\text{on\_count}(n)))$ 
4: Compute Z-scores of log-transformed drop-off counts:  $z_n^{\text{off}} \leftarrow$ 
    $\text{Zscore}(\log(\text{off\_count}(n)))$ 
5: for each node  $n \in \mathcal{N}$  do
6:   if  $z_n^{\text{on}} \geq z_{\text{threshold}}$  then
7:      $\text{is\_high\_demand}(n) \leftarrow 1$ 
8:   else
9:      $\text{is\_high\_demand}(n) \leftarrow 0$ 
10:  end if
11:  if  $z_n^{\text{off}} \geq z_{\text{threshold}}$  then
12:     $\text{is\_high\_attraction}(n) \leftarrow 1$ 
13:  else
14:     $\text{is\_high\_attraction}(n) \leftarrow 0$ 
15:  end if
16: end for

```

References

- [1] S. Oh, R. Seshadri, C. L. Azevedo, N. Kumar, K. Basak, M. Ben-Akiva,
Assessing the impacts of automated mobility-on-demand through
agent-based simulation: A study of singapore, Transportation Research

- Part A: Policy and Practice 138 (2020) 367–388. doi:10.1016/j.tra.2020.06.004.
- [2] A. Siddiq, T. A. Taylor, Ride-hailing platforms: Competition and autonomous vehicles, *Manufacturing & Service Operations Management* 24 (3) (2022) 1511–1528. doi:10.1287/msom.2021.1013.
- [3] L. Rayle, D. Dai, N. Chan, R. Cervero, S. Shaheen, Just a better taxi? a survey-based comparison of taxis, transit, and ridesourcing services in san francisco, *Transport Policy* 45 (2016) 168–178. doi:10.1016/j.tranpol.2015.10.004.
- [4] Á. Aguilera-García, J. Gómez, G. Velázquez, J. M. Vassallo, Ridesourcing vs. traditional taxi services: Understanding users’ choices and preferences in spain, *Transportation Research Part A: Policy and Practice* 155 (2022) 161–178. doi:10.1016/j.tra.2021.11.002.
- [5] W. Ge, Taxi operational characteristics and development policy in shanghai, *Urban Transport of China* 15 (2) (2017) 60–66. doi:10.13813/j.cn11-5141/u.2017.0209.
- [6] Shanghai statistical bulletin on national economic and social development 2024, Tech. rep., Shanghai Municipal Bureau of Statistics, <https://tjj.sh.gov.cn/tjgb/20250324/a7fe18c6d5c24d66bfca89c5bb4cdcfb.html> (March 2025).
- [7] A. Henao, W. E. Marshall, The impact of ride-hailing on vehicle miles traveled, *Transportation* 46 (6) (2019) 2173–2194. doi:10.1007/s11116-018-9923-2.

- [8] G. D. Erhardt, S. Roy, D. Cooper, B. Sana, M. Chen, J. Castiglione, Do transportation network companies decrease or increase congestion?, *Science Advances* 5 (5) (2019) eaau2670. doi:10.1126/sciadv.aau2670.
- [9] Z. Wang, Y. Zhang, B. Jia, Z. Gao, Comparative analysis of usage patterns and underlying determinants for ridehailing and traditional taxi services: A chicago case study, *Transportation Research Part A: Policy and Practice* 179 (2024) 103912. doi:10.1016/j.tra.2023.103912.
- [10] A. Brown, W. LaValle, Hailing a change: Comparing taxi and ridehail service quality in los angeles, *Transportation* 48 (2) (2021) 1007–1031. doi:10.1007/s11116-020-10086-z.
- [11] I. O. Olayode, A. Severino, F. J. Alex, E. Macioszek, L. K. Tartibu, Systematic review on the evaluation of the effects of ride-hailing services on public road transportation, *Transportation Research Interdisciplinary Perspectives* 22 (2023) 100943. doi:10.1016/j.trip.2023.100943.
- [12] R. G. McKane, D. J. Hess, The impact of ridesourcing on equity and sustainability in north american cities: A systematic review of the literature, *Cities* 133 (2023) 104122. doi:10.1016/j.cities.2022.104122.
- [13] Y. Li, D. A. Vignon, Do ride-hailing congestion fees in nyc work?, *Transportation Research Part A: Policy and Practice* 190 (2024) 104274. doi:10.1016/j.tra.2024.104274.
- [14] H. Wang, H. Yang, Ridesourcing systems: A framework and review, *Transportation Research Part B: Methodological* 129 (2019) 122–155. doi:10.1016/j.trb.2019.07.009.

- [15] R. G. McKane, D. J. Hess, The impact of ridesourcing on equity and sustainability in north american cities: A systematic review of the literature, *Cities* 133 (2023) 104122. doi:10.1016/j.cities.2022.104122.
- [16] M. Vega-Gonzalo, Álvaro Aguilera-García, J. Gómez, J. M. Vassallo, Traditional taxi, e-hailing or ride-hailing? a gsem approach to exploring service adoption patterns, *Transportation* 51 (4) (2023) 1239–1278. doi:10.1007/s11116-022-10356-y.
- [17] D. Q. Nguyen-Phuoc, coauthors, The formation of passenger loyalty: Differences between ride-hailing and traditional taxi services, *Travel Behaviour and Society* 24 (2021) 218–230. doi:10.1016/j.tbs.2021.08.005.
- [18] G. Zhai, K. Xie, H. Yang, D. Yang, Are ride-hailing services safer than taxis? a multivariate spatial approach with accommodation of exposure uncertainty, *Accident Analysis & Prevention* (2023). doi:10.1016/j.aap.2023.107281.
- [19] Y. Luo, A. Huang, Z. He, J. Zeng, D. Wang, Exploring competitiveness of taxis to ride-hailing services from a multidimensional spatio-temporal perspective: A case study in beijing, china, *Journal of Transport Geography* 118 (2024) 103936. doi:10.1016/j.jtrangeo.2024.103936.
- [20] J. Li, Z. Xiong, H. Wu, Understanding operation patterns of urban online ride-hailing services: A case study of xiamen, *Transport Policy* 101 (2020) 100–118. doi:10.1016/j.tranpol.2020.12.008.

- [21] J. Soria, Y. Chen, A. Stathopoulos, K-prototypes segmentation analysis on large-scale ridesourcing trip data, *Transportation Research Record* 2674 (9) (2020) 383–394. doi:10.1177/0361198120929338.
- [22] X. Iogansen, Y. Lee, M. Young, J. Compostella, G. Circella, A. Jenn, Ride-hailing use, travel patterns and multimodality: A latent-class cluster analysis of one-week gps-based travel diaries in california, *Travel Behaviour and Society* 38 (3) (2025). doi:10.1016/j.tbs.2024.100855.
- [23] M. M. Vazifeh, P. Santi, G. Resta, S. H. Strogatz, C. Ratti, Addressing the minimum fleet problem in on-demand urban mobility, *Nature* 557 (2018) 534–538. doi:10.1038/s41586-018-0095-1.
- [24] G. Feng, G. Kong, Z. Wang, We are on the way: Analysis of on-demand ride-hailing systems, *Manufacturing & Service Operations Management* 23 (5) (2021) 1237–1256. doi:10.1287/msom.2020.0880.
- [25] S. Feng, T. Chen, Y. Zhang, J. Ke, Z. Zheng, H. Yang, A multi-functional simulation platform for on-demand ride service operations, *Communications in Transportation Research* 4 (2024) 100141. doi:10.1016/j.commtr.2024.100141.
- [26] S. R. Balseiro, D. B. Brown, C. Chen, Pricing and optimization in shared vehicle systems: A queueing-theoretic approach, *Manufacturing & Service Operations Management* 22 (4) (2020) 851–867. doi:10.1287/msom.2020.0895.
- [27] C. V. Beojone, N. Geroliminis, On the inefficiency of ridesourcing services towards urban congestion, *Transportation Research Part C*:

- Emerging Technologies 124 (2021) 102890. doi:10.1016/j.trc.2021.102890.
- [28] A. Siddiq, T. A. Taylor, Ride-hailing platforms: Competition and autonomous vehicles, *Manufacturing & Service Operations Management* 24 (3) (2022) 1511–1528. doi:10.1287/msom.2021.1013.
- [29] Y. Liang, Q. Yuan, D. Wang, Y. Feng, P. Xu, J. Zhou, Panacea or placebo? exploring causal effects of nonlocal vehicle driving restriction policies on traffic congestion using difference-in-differences approach, *Transportation* 51 (6) (2023) 2253–2275. doi:10.1007/s11116-023-10404-1.
- [30] Y. Liang, B. Yu, X. Zhang, Y. Lu, L. Yang, The short-term impact of congestion taxes on ridesourcing demand and traffic congestion: Evidence from chicago, *Transportation Research Part A: Policy and Practice* 172 (2023) 103661. doi:10.1016/j.tra.2023.103661.
- [31] C. Yan, H. Zhu, N. Korolko, D. Woodard, Dynamic pricing and matching in ride-hailing platforms, *Naval Research Logistics* 67 (8) (2020) 705–724. doi:10.1002/nav.21872.
- [32] N. Garg, H. Nazerzadeh, Driver surge pricing, *Management Science* 68 (5) (2022) 3219–3235. doi:10.1287/mnsc.2021.4058.
- [33] C. Riley, P. Van Hentenryck, E. Yuan, Real-time dispatching of large-scale ride-sharing systems: Integrating optimization, machine learning, and model predictive control, in: *Proceedings of the Twenty-Ninth International Joint Conference on Artificial Intelligence (IJCAI-20)*, Special

Track on AI for Computational Sustainability and Human Well-being, 2020, pp. 4417–4423. doi:10.24963/ijcai.2020/609.

- [34] R. Jonker, T. Volgenant, Improving the hungarian assignment algorithm, *Operations Research Letters* 5 (4) (1986) 171–175. doi:10.1016/0167-6377(86)90073-8.
- [35] F. Guo, D. Zhang, Y. Dong, Z. X. Guo, Urban link travel speed dataset from a megacity road network, *Scientific Data* 6 (2019) 61. doi:10.1038/s41597-019-0060-3.
- [36] S. Ruder, An overview of gradient descent optimization algorithms, *arXiv preprint arXiv:1609.04747* (2016).
- [37] R. W. Floyd, Algorithm 97: Shortest path, *Communications of the ACM* 5 (6) (1962) 345.
- [38] C. D. Cauwer, J. V. Mierlo, T. Coosemans, Energy consumption prediction for electric vehicles based on real-world data, *Energies* 8 (8) (2015) 8573–8593. doi:10.3390/en8088573.
- [39] Roland Berger Strategy Consultants, Think act: Urban mobility in the age of mobile internet (May 2015).
URL <https://www.rolandberger.com.cn>
- [40] P. C. Jones, The fleet design problem, *The Engineering Economist* 39 (1) (1993) 1–15. doi:10.1080/00137919308903089.
- [41] Ministry of Transport of the People’s Republic of China, Guiding opinions on deepening reform and advancing the healthy development

of the taxi industry (2016).

URL https://www.gov.cn/xinwen/2016-07/28/content_5097333.htm

- [42] D. J. Sun, X. Ding, Spatiotemporal evolution of ridesourcing markets under the new restriction policy: A case study in shanghai, *Transportation Research Part A: Policy and Practice* 130 (2019) 227–239. doi:10.1016/j.tra.2019.09.052.
- [43] Y. Liang, H. L. et al., Meituan’s real-time intelligent dispatching algorithms build the world’s largest minute-level delivery network, *INFORMS Journal on Applied Analytics* 54 (1) (2024) 84–101. doi:10.1287/inte.2023.0084.